Texture and Scale in Object-Based Analysis of Subdecimeter Resolution Unmanned Aerial Vehicle (UAV) Imagery

Andrea S. Laliberte and Albert Rango

***Abstract*—Imagery acquired with unmanned aerial vehicles (UAVs) has great potential for incorporation into natural resource monitoring protocols due to their ability to be deployed quickly and repeatedly and to fly at low altitudes. While the imagery may have high spatial resolution, the spectral resolution is low when lightweight off-the-shelf digital cameras are used, and the inclusion of texture measures can potentially increase the classification accuracy. Texture measures have been used widely in pixel-based image analysis, but their use in an object-based environment has not been well documented. Our objectives were to determine the most suitable texture measures and the optimal image analysis scale for differentiating rangeland vegetation using UAV imagery segmented at multiple scales. A decision tree was used to determine the optimal texture features for each segmentation scale. Results indicated the following: 1) The error rate of the decision tree was lower; 2) prediction success was higher; 3) class separability was greater; and 4) overall accuracy was higher (high 90% range) at coarser segmentation scales. The inclusion of texture measures increased classification accuracies at nearly all segmentation scales, and entropy was the texture measure with the highest score in most decision trees. The results demonstrate that UAVs are viable platforms for rangeland monitoring and that the drawbacks of low-cost off-the-shelf digital cameras can be overcome by including texture measures and using object-based image analysis which is highly suitable for very high resolution imagery.**

***Index Terms*—Object-based classification, rangelands, scale, texture, unmanned aircraft.**

I. Introduction

REMOTE SENSING data and image analysis tools have become an integral part of rangeland mapping, assessment, and monitoring in recent years. While satellite imagery and aerial photography have been used for these tasks [1], imagery acquired with unmanned aerial vehicles (UAVs) offers several advantages. UAVs can be deployed quickly and repeatedly and are less costly and safer than piloted aircraft. UAVs can also obtain subdecimeter resolution imagery. These advantages make UAVs ideal for use in forest fire applications and other natural disasters [2], particularly if orthoimagery can be produced in near real time, and with high accuracy [3].

In rangelands, UAV imagery provides the ability to quantify spatial patterns and patches of vegetation and soil not detectable with piloted aircraft or satellite imagery [4], [5]. The questions that ecosystem modelers and agencies charged with evaluating rangeland health are attempting to solve cannot be answered with the comparatively lower resolution of imagery from piloted aircraft. UAV imagery, on the other hand, offers the ability to detect and map spatial characteristics of vegetation and gaps between vegetation patches associated with erosion risk and wildlife habitat quality [5].

Due to low payload capabilities of small- and medium-size UAVs, imagery is often acquired with inexpensive off-the-shelf digital cameras. While the spatial resolution of this imagery is high, the spectral resolution is not, and imagery usually lacks a near-infrared band. For that reason, texture can be a potentially useful parameter for mapping rangeland vegetation and soils with this imagery.

Texture measures have been used extensively in remote sensing, particularly with high and very high resolution images and with panchromatic imagery [6]. In general, classification accuracies are improved by the use of texture [7]–[10]. Commonly used texture measures are second-order statistics derived from the gray-level cooccurrence matrix (GLCM). These statistics describe changes in gray-level values of pixels and relationships between pixel pairs in a given area [11]. Texture is a statistical measure of structure and can be defined as smooth when the within-class variability is lower than the between-class variability. Likewise, texture is coarse when the within-class variability is similar to or greater than the between-class variability [12]. This property makes texture useful for differentiating relatively smooth surfaces in an image (water or bare ground) from coarser more textured surfaces (urban or vegetated areas). With a fine enough resolution, lower textured grass areas can be differentiated from higher textured shrubs, which contain a larger amount of shadow pixels.

In pixel-based analysis, texture is calculated with moving windows and suffers from the boundary problem, because windows can straddle the boundary between two landscape features and potentially different textures. This boundary problem increases with texture window size [10]. When texture is calculated from segmented imagery, as is done in object-based

Manuscript received December 12, 2007; revised June 13, 2008, August 26, 2008, and September 30, 2008. First published February 3, 2009; current version published February 19, 2009. This work was supported in part by the USDA Agricultural Research Service and the National Science Foundation Long-Term Ecological Research Program, Jornada Basin IV: Linkages in Semiarid Landscapes, and in part by the USDA Natural Resources Conservation Service in support of the Conservation Effects Assessment Program.

A. S. Laliberte is with the Jornada Experimental Range, New Mexico State University, Las Cruces, NM 88003 USA (e-mail: alaliber@nmsu.edu).

A. Rango is with the USDA-ARS Jornada Experimental Range, New Mexico State University, Las Cruces, NM 88003 USA (e-mail: alrango@nmsu.edu).

Digital Object Identifier 10.1109/TGRS.2008.2009355

image analysis [13], the boundary problem is minimized [14], because the segments are relatively homogenous and texture is calculated per segment.

Object-based image analysis has proven to be successful and is often superior to pixel-based analysis with high and very high resolution images that exhibit a large amount of shadow, low spectral information, or a low signal-to-noise ratio [15], [16]. We used an object-based image analysis approach (eCognition, now called Definiens Professional [13]) for mapping shrubs with multispectral and panchromatic aerial photos [17] and for mapping arid rangeland vegetation with QuickBird imagery [18]. Analysis of UAV imagery with the same approach demonstrated the ability to map small shrubs (30-cm diameter) and to differentiate different types of bare soil and different densities of grass cover [5].

In object-based image analysis, the analyst is faced with two main challenges. The first challenge is the determination of segmentation parameters, particularly the segmentation scale. Because the segmentation parameters depend on both image resolution and the objects of interest to be mapped, often, trial and error, as well as visual analysis, is used to find acceptable values [19]–[21]. An optimal scale parameter can be determined by using class separability indices [22] or by analyzing local variance [23]. In many cases, multiple segmentation scales are used to map detailed features at a fine segmentation scale and broader features at a coarser segmentation scale [18], [24]–[26]. In [27], the authors used a hierarchical segmentation as a preprocessing tool for improving the subsequent feature extraction process, which was driven by relationships of objects at multiple scales. However, in this paper, our goal was to find a single segmentation scale that would best separate bare ground, shrubs, and grasses.

The second challenge is the determination of suitable features for classification. In Definiens Professional, as in other object-based image analysis software packages, potentially hundreds of spectral, spatial, and contextual features are available for classification, and often, visual analysis or prior knowledge is used to choose features subjectively. Due to their complexity, texture measures such as GLCM are time-consuming to calculate and display in an object-based environment, particularly at fine segmentation scales. In addition, if a high-dimensional feature space is used (such as all the texture measures), the class samples have to be sufficient in number to create a reliable covariance matrix [28]. This is often prohibitive.

A faster and more objective tool for feature selection is a decision tree, because it is a nonparametric statistical technique that is not affected by outliers and correlations, it can reveal variable interactions, and it is an excellent data reduction tool. In a decision tree, a data set is successively split into increasingly homogenous subsets until terminal nodes are determined [29]. A common splitting rule in decision trees (and used in this paper) is the Gini index, a measure of heterogeneity. If all observations in a node belong to the same class, the Gini index is zero; when different class sizes at the node are equal, the index is one [29]. Decision tree results can be used by applying the derived class prediction rules or by using the decision trees as a feature selection tool. We used the latter application in this paper and performed classification within the object-based environment using a fuzzy classification approach.

Fig. 1. BAT 3 UAV on catapult launcher ready for takeoff.

Decision trees are commonly used for remote sensing applications and often reduce the classification error [30], [31]. Decision trees are also increasingly used in combination with object-based image analysis due to their data reduction capabilities [16], [18], [24], [32], [33].

In this paper, our objectives were to determine the optimal segmentation scale and most suitable texture measures for differentiating bare ground, shrubs, and herbaceous vegetation in an arid rangeland using unmanned aircraft imagery. Results are designed to be incorporated into a workable solution for rangeland monitoring protocols using UAVs.

II. Methods

A. Study Area and Data Collection

The imagery was acquired in October 2006 at the Jornada Experimental Range in southern New Mexico in the northern portion of the Chihuahuan desert. For this study, we selected an area depicting a set of constructed shallow dikes designed to retain water and promote vegetation growth. The chosen site was a mixture of vegetation and areas of bare ground of various soils. Dominant shrubs in the study area consisted of tarbush (*Flourensia cernua*), honey mesquite (*Prosopis glandulosa*), and broom snakeweed (*Gutierrezia sarothrae*), and dominant grasses were bluestem (*Bothriochloa laguroides*), dropseed species (*Sporobolus* spp.), and burrograss (*Scleropogon brevifolius*).

The imagery was acquired with an MLB BAT 3 UAV. The BAT system consists of a fully autonomous GPS-guided UAV (10-kg weight), a catapult launcher, ground station with mission planning and flight software, and telemetry system (Fig. 1). The aircraft was equipped with a Canon SD 550 seven-megapixel digital camera and flew at 150 m above ground, acquiring imagery with 60% forward lap and 30% sidelap. The resulting image footprints were 152 m $\times$ 114 m and had a pixel size of 5 cm. Eight images covering the dike area were orthorectified using Leica Photogrammetric Suite 9.0 (Leica Geosystems Geospatial Imaging LLC) with a root mean square error of 0.33 pixels and mosaicked into a single image. Brightness differences between the images were minor, and no color

balancing was required. Due to the object-based image analysis approach used, minor changes in brightness values do not affect the analysis, because individual pixels are aggregated into image objects.

Ground data collection consisted of using a randomly selected location, with a differentially corrected GPS, and delineating 300 samples, 100 for each of the three classes of interest (bare ground, shrubs, and grass) in polygon format. Because of the object-based approach, samples in polygon format are more appropriate than point locations [18]. In addition, because of GPS error and the 5-cm resolution imagery, it is not possible to relate GPS data to a single pixel. The average size of the polygons was 56.1 m^2 (SD: 5.2 m^2) for bare ground, 16.3 m^2 (SD: 2.5 m^2) for grass, and 3.7 m^2 (SD: 0.6 m^2) for shrubs. The difference in average size for each class was due to relatively small patches of grass and the size of shrubs in this vegetation community. Half of the samples were used for mapping purposes, and half were retained for accuracy analysis.

B. Image Processing

The general workflow consisted of the following: 1) segmenting the image at multiple scales; 2) selecting suitable texture measures to separate the three classes of interest by using a decision tree; and 3) determining class separability as well as classification accuracy with and without the selected texture measures. The image was segmented using Definiens Professional 5 [13]. Three segmentation parameters have to be selected: scale parameter, color (spectral information), and shape. The scale parameter is unitless and controls the general size of image objects. A smaller scale parameter results in smaller image objects. Color and shape are weighted from zero to one, and smoothness and compactness, which are part of the shape setting, can also be weighted from zero to one. The segmentation is a bottom-up region merging technique, whereby smaller segments are merged into larger ones based on heterogeneity (similarity of spectral and spatial characteristics) of adjacent image objects and controlled by the three segmentation parameters [34].

Based on previous research in similar vegetation [5], [17], [18], color/shape and compactness/smoothness were set to 0.9/0.1 and 0.5/0.5, respectively. The image was segmented at 15 segmentation scales starting with scale parameter 10 and ending with 80 in increments of 5 (Fig. 2). Scale 80 was used as the coarsest scale, because we wanted to retain individual shrubs, and at a coarser scale than 80, shrubs were being merged into broader image objects. The segmentation statistics are shown in Table I.

C. Texture Features

In pixel-based analysis, GLCM statistics are computed for a chosen pixel window (3×3, 5×5, etc.), while in object-based image analysis as implemented in Definiens Professional 5, the image is segmented first, using only the red, green, and blue (RGB) values, then texture features are calculated for the image objects. Border effects are reduced by taking into account pixels that border the image object [13].

We used eight GLCM statistics and two gray-level difference vector (GLDV) statistics in this paper. The GLDV is a sum of the diagonals of the GLCM and a measure of the absolute differences of neighbors. We used the average of the three input bands and the average of the four possible directions to be calculated due to the assumption that bare soil, shrubs, and grass are not directionally biased.

The texture measures used were homogeneity $(MHOM)$, contrast $(MCON)$, dissimilarity $(MDIS)$, entropy $(MENT)$, angular second moment $(MASM)$, mean $(MMEAN)$, standard deviation $(MSTD)$, correlation $(MCOR)$, GLDV angular second moment $(VASM)$, and GLDV entropy $(VENT)$. The statistics are defined as follows:

$$MHOM = \sum_{i,j=0}^{N-1} \frac{P_{i,j}}{1+(i-j)^2} \tag{1}$$

$$MCON = \sum_{i,j=0}^{N-1} P_{i,j}(i-j)^2 \tag{2}$$

$$MDIS = \sum_{i,j=0}^{N-1} P_{i,j}|i-j| \tag{3}$$

$$MENT = \sum_{i,j=0}^{N-1} P_{i,j}(-\ln P_{i,j}) \tag{4}$$

$$MASM = \sum_{i,j=0}^{N-1} P_{i,j}^2 \tag{5}$$

$$MMEAN = \frac{\sum_{i,j=0}^{N-1} P_{i,j}}{N^2} \tag{6}$$

$$MSTD = \sqrt{\sigma_i^2};\ \sqrt{\sigma_j^2}, \qquad \text{where}$$

$$\sigma_i^2 = \sum_{i,j=0}^{N-1} P_{i,j}(i-\mu_i)^2$$

$$\sigma_j^2 = \sum_{i,j=0}^{N-1} P_{i,j}(j-\mu_j)^2 \tag{7}$$

$$MCOR = \sum_{i,j=0}^{N-1} P_{i,j}\frac{(i-\mu_i)(j-\mu_j)}{\sigma_i\sigma_j} \tag{8}$$

$$VASM = \sum_{k=0}^{N-1} V_k^2 \tag{9}$$

$$VENT = \sum_{k=0}^{N-1} V_k(-\ln V_k) \tag{10}$$

where $P_{i,j}$ is the normalized gray-level value in the cell i, j of the matrix, N is the number of rows or columns, σ_i and σ_j are the standard deviations of row i and column j, μ_i and μ_j are

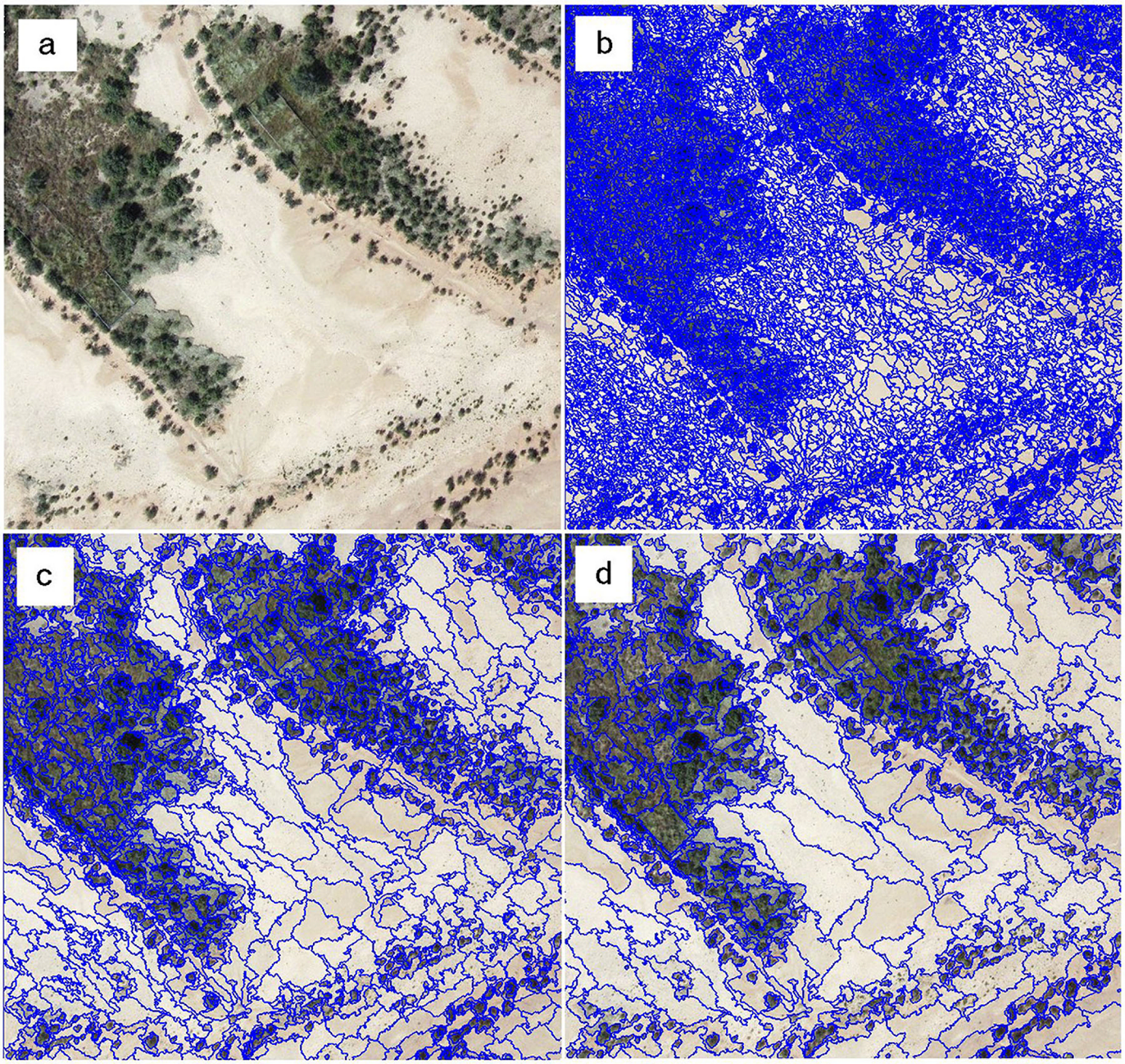

Fig. 2. Image segmentations of UAV image mosaic, showing (a) 100-m × 100-m area of the aerial photo mosaic, (b) finest segmentation at scale parameter 10, (c) intermediate segmentation at scale parameter 45, and (d) coarsest segmentation at scale parameter 80.

the means of row i and column j, V_k is the normalized GLDV, and $k = |i - j|$. Every GLCM is normalized according to

$$P_{i,j} = \frac{C_{i,j}}{\sum_{i,j=0}^{N-1} C_{i,j}} \tag{11}$$

where $C_{i,j}$ is the value of the cell i, j of the matrix.

D. Decision Tree Analysis

The concept behind a decision tree analysis is the successive splitting of the data set into increasingly homogenous subsets until terminal nodes are determined. In this paper, the response variables were the vegetation classes, and the explanatory variables were the texture values for the sample objects. Texture values for each of the sample objects for the three classes were calculated and imported into the decision tree analysis software CART by Salford Systems, which implements the algorithm developed by Clausi [28]. The Gini index [35], a measure of heterogeneity, was used as the splitting rule. Initially, a maximal tree was grown and then pruned back to obtain an optimal tree by using tenfold cross-validation. In this process, a maximal tree is grown from 90% of the subsamples, and 10% of samples are reserved for assessing the misclassification error. This process was repeated ten times, each time reserving a different 10% for error assessment. The optimal tree is the one with the lowest misclassification error. This analysis was performed for each segmentation level.

TABLE I
NUMBER OF OBJECTS AND MEAN OBJECT SIZE FOR 15 SEGMENTATION SCALES

Scale	Number of objects	Mean object size (m^2)
10	265484	0.33
15	122160	0.79
20	68644	1.71
25	43911	3.00
30	30596	5.26
35	22627	8.18
40	17573	11.46
45	14085	14.19
50	11505	17.98
55	9704	20.89
60	8291	23.66
65	7157	26.40
70	6189	29.97
75	5420	36.33
80	4851	42.29

We identified the optimal texture measures at each segmentation scale by assessing variable importance. Prediction success, cross-validated error rate of the tree, and terminal node purity, in conjunction with class separability and accuracy from additional analysis, served as an indication of the optimal segmentation scale for our data. We were also interested in determining whether different texture measures dominated at finer or coarser segmentation scales, and if one or few texture measures would be suitable at most segmentation scales.

Correlations between texture measures have been reported for several studies in pixel-based analysis [28], [36]–[38], but not for object-based analysis. While correlation between variables is not a large concern in decision tree analysis, a classification with multiple texture measures in Definiens Professional is computer intensive, and fewer variables are preferred. For that reason, correlation between texture measures was analyzed using Spearmean's rank correlation coefficient, which does not require the assumptions of normality and linearity [39].

E. Classification Accuracy and Class Separability

Definiens Professional implements a fuzzy classification approach, whereby the outcome of a classification describes the degree of membership to a specific class. The membership ranges from zero (no assignment) to one (full assignment). The closer an image object is located in feature space to a sample of a class, the higher the membership degree is to this class. The distance d between sample object s and image object o is computed as follows:

$$d = \sqrt{\sum_f \left(\frac{v_f^s - v_f^o}{\sigma_f} \right)^2} \tag{12}$$

where

v_f^s feature value of a sample object for feature f;
v_f^o feature value of an image object for feature f;
σ_f standard deviation of the feature values for feature f.

In order to convert the fuzzy classification results to a final map with discrete classes, the class with the highest membership degree is chosen for the final class assignment. The error matrix is based on samples that represent image objects, but is expressed in pixels. Classification accuracies (overall, producers, and users) and the Kappa Index of Agreement (KIA) [40] were calculated for each segmentation scale for classifications using only the RGB bands as well as using the RGB bands plus the texture measures selected by the decision tree. This allowed us to assess how much the classification was improved by addition of texture features.

Separation distances between the classes are calculated in Definiens Professional by determining for each sample of class a the sample of class b with the smallest Euclidean distance to it. This is repeated for samples of class b compared to class a, etc. The Euclidean distances are then averaged over all samples. Separation distances were calculated using the following: 1) only the RGB bands and 2) using the RGB bands plus the texture measures suggested by the decision tree for the respective segmentation scales.

III. RESULTS

A. Decision Tree Results

The optimal texture features selected by the decision tree varied for the segmentation scales; however, we observed several trends. Table II shows the variable importance ranking for the decision trees for each segmentation scale. Variable importance is reported as a score in CART, ranging from 0 to 100, and it reflects the contribution each variable makes in predicting the target variable [35]. A score of 100 indicates the first splitter in the tree. As the scale became coarser, fewer texture measures were required by the tree to partition the classes. From scales 65 to 80, the same three texture measures ($MENT$, $MCON$, and $MSTD$) were chosen in the same order and with similar scores. $MENT$ most frequently received a score of 100, and it was the texture measure chosen in every tree. In addition, it ranked either first or second from scales 15 to 80. At finer scales (10–40), $MSTD$, $MDIS$, or $MCON$ had the highest scores.

In a decision tree, the cross-validated relative cost (CVRC) is the misclassification or error rate of the tree, based on using the tenfold cross-validation method in this paper. For each segmentation scale, the tree with the lowest CVRC was chosen, as is common in decision tree analysis. If a tree has a CVRC of 0.25, it is interpreted as an error rate of 25% [35], meaning that lower values of CVRC are desired. Results indicated that the CVRC decreased from 60% at scale 10 to the lowest value of 20% at scale 60.

The prediction success for the cross-validated samples also indicated that segmentation scales at or near 60 appeared to be most appropriate for this data set. Prediction success is calculated similar to an error matrix, comparing the training samples to the cross-validated samples in CART. At scales 10–30, the prediction success varied greatly for the three classes of interest. At and beyond scale 35, the prediction success was comparable for all the classes. The classes reached their highest prediction success at scales 60 for grass, 75 for shrubs, and 80 for bare, while the overall prediction success peaked at scale 60 (Fig. 3).

TABLE II
VARIABLE IMPORTANCE, REPORTED AS SCORES FROM CART, FOR 15 SEGMENTATION SCALES. A SCORE OF 100 INDICATES THE FIRST SPLITTER OR MOST IMPORTANT VARIABLE IN THE DECISION TREE

Scale	MENT	MMEAN	MCOR	MCON	MHOM	MDIS	MSTD	VENT
10	37.92	27.89	10.15	6.36	6.19		100.00	43.96
15	49.44		24.19		11.43	100.00		33.72
20	46.11			100.00			15.30	
25	77.04	23.78	10.88	100.00			28.74	8.90
30	74.08	18.74	18.26			100.00	100.00	37.75
35	86.56	28.26	13.85			41.84	100.00	
40	95.61			47.88			16.36	
45	100.00	8.08	6.66	91.19	6.51	4.92		
50	99.06					100.00		
55	100.00					96.85		
60	100.00					95.11		
65	100.00	6.80		94.05			38.33	
70	100.00			96.05		8.15	87.91	
75	100.00			68.33			67.76	
80	100.00			73.30			70.29	

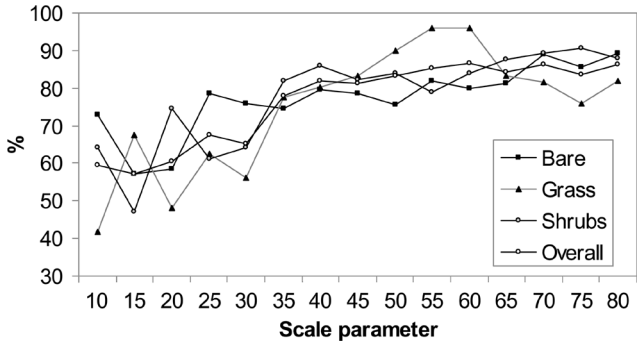

Fig. 3. Prediction success of decision trees for 15 segmentation scales.

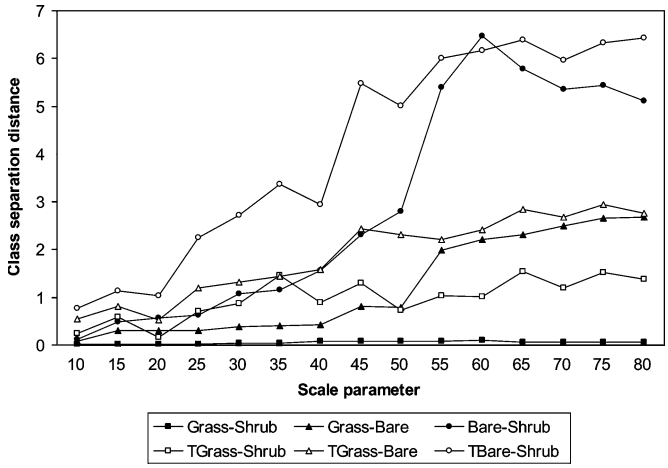

Fig. 4. Class separation distances for three class combinations using only RGB bands (closed symbols) and using RGB bands plus texture measures selected by the decision tree (open symbols).

The terminal node purity is another measure for assessing a decision tree. Terminal node purity shows the homogeneity of the terminal nodes of the decision trees and is an indication of how well CART partitions the classes. In general, fewer nodes with higher node purity are preferable to many nodes of lower purity. It is also desirable that all classes show similar values of node purity, which indicates a better classification based on the decision tree. Terminal node purity followed a similar trend as prediction success, with overall higher node purity above 88% for scales 55 and coarser. At scale 65 and above, node purity was above 90% for all classes with the exception of shrubs at scale 75. The number of nodes in the decision tree gradually dropped from a high of 15 at scale 10 to 3 nodes at scales 50–60, after which nodes increased to 7 and then fell again to 4 at the coarsest scale.

$MCOR$, $MMEAN$, and $MENT$ were the three measures showing the least correlation with other texture measures. At finer segmentation scales (below 20–25), correlation coefficients often changed at a greater rate from one scale to the next, while at coarser segmentation scales, the rate of change in correlation coefficient was smaller. The highest correlation coefficients that remained stable across all scale parameters were found for $MCON$–$MDIS$ and $VASM$–$VENT$.

B. Classification Accuracy and Class Separability

For all three class comparisons, class separability increased with increasing segmentation scale, although for grass–shrub using RGB bands only, this increase was minimal (and not visible on the graph at that scale) (Fig. 4). This behavior occurred for RGB bands only as well as RGB bands plus texture. In addition, when texture measures were included, class separability was always greater than that for RGB bands alone. This held true for all three class comparisons, with only one exception for bare–shrub at scale 60. There was a noticeable increase in separability after scale 40, particularly for bare–shrub. Maximum separability for bare–shrub occurred at scale 80, for grass–bare at scale 75, and for grass–shrub at scale 65 (values for RGB+texture).

Similar to the class separability results, the overall accuracy and KIA increased with increasing segmentation scale for both RGB and RGB+texture (Fig. 5). The inclusion of texture increased the accuracy measures at all segmentation scales with the exception of the coarsest scale 80, at which the accuracy of RGB+texture was lower (92.25%) than the accuracy of RGB bands alone (95.19%). In general, accuracy percentages and KIA values were relatively high for both RGB and RGB+texture, which is not surprising given the image resolution and the fact that we only analyzed three classes. Accuracies of producers and users showed confusion between

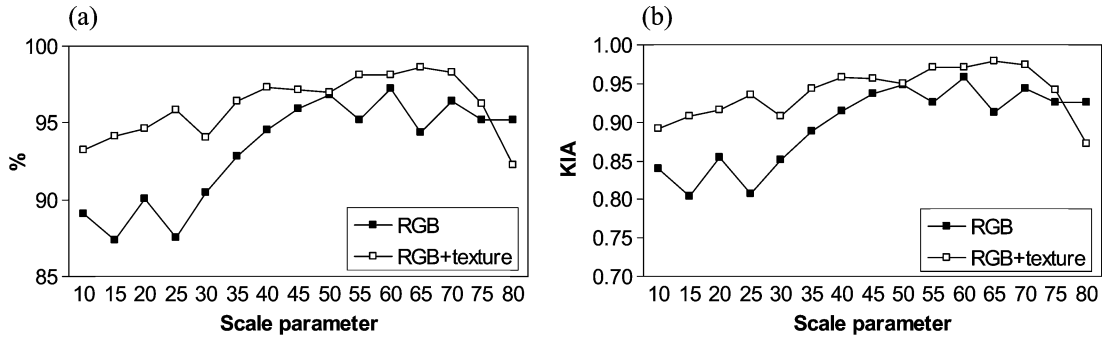

Fig. 5. Accuracy assessment graphs for classification of UAV image into bare, grass, and shrub, showing (a) overall accuracy in percent and (b) KIA, for RGB bands only (closed symbols) and RGB bands plus texture (open symbols).

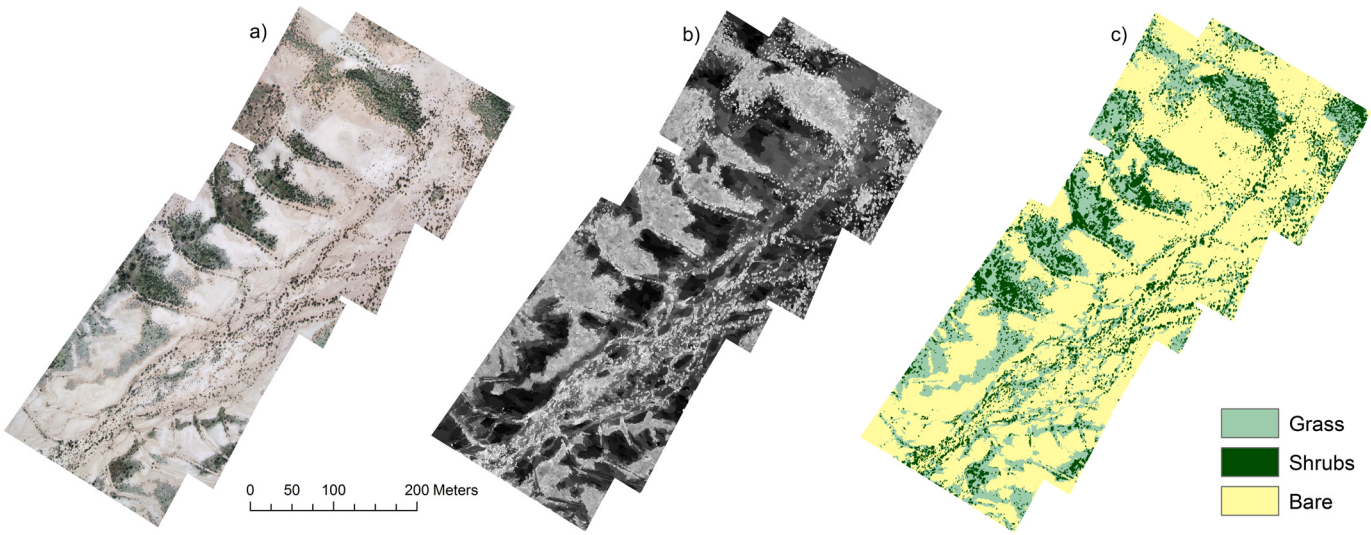

Fig. 6. (a) Image mosaic, (b) entropy image, and (c) classification result at scale parameter 60.

grass and shrub until scale 40 was reached, after which both producers' and users' accuracies were consistently over 80%, with the only exception at scale 80, where producers' accuracy of shrubs dropped to 65% (RGB+texture). Both producers' and users' accuracies for bare were consistently over 95%, with the majority of values nearing 100%. The classification for scale 60 is shown in Fig. 6.

IV. Discussion

The results of this paper give a strong indication that a segmentation scale greater than 40 is most appropriate for differentiating bare, grass, and shrub classes with UAV imagery in this arid rangeland. The results from the decision tree analysis corroborate the results of the accuracy analysis: The error rate of the decision tree was lower, prediction success was higher, class separability was greater, and overall accuracy and KIA were higher in >40 than in <40 scale parameters. Taking into account all results, the optimal scale parameters lie between 55 and 70 for this data set. This is also confirmed by visual assessment, and if a single scale would be chosen, we would select scale 60. While the absolute number of the scale parameter changes with image resolution and classes of interest, the knowledge that a relatively coarser segmentation is more appropriate than a finer one is important. Based on previous studies with aerial photos from piloted and unmanned aircraft [5], [17] and QuickBird imagery [18] in this area, we know that there is a tendency to segment an image at a finer scale than the outcome of this study would indicate. This may be due to the analyst's familiarity with the pixel-based analysis, or the tendency to want to capture every single shrub or grass patch, or the belief that image objects can always be aggregated to a coarser scale if needed.

Determining the optimal scale parameter is of utmost importance in the object-based image analysis and, recently, has been the topic of various studies [18], [22], [23]. An optimal scale parameter is particularly important in studies such as ours, where a single segmentation scale is used as a first assessment of broad vegetation classes. We acknowledge that for more detailed classifications, multiple segmentation scales may be better suited so that vegetation patches could be mapped at different scales and shrubs of different sizes could be classified at greater detail.

Closer inspection of the imagery showed why the relatively coarser scale parameters led to higher accuracy. At scales of <40, image objects were quite small and individual grass and shrub patches consisted of multiple image objects. As the scale increased, those patches, particularly shrubs, were delineated more accurately and completely. At the coarsest scales, however, small shrubs were lost because they were more likely

to be incorporated into neighboring objects (Fig. 2). Because portions of shrub and grass patches may be relatively similar spectrally and even with regard to texture, classification accuracy and class separability increased when those objects were delineated more accurately, which occurred at segmentation scales between 40 and 70.

As the study in [23] had shown, as objects are aggregated with increasing segmentation, average local variance increases, then levels out, and the authors used this behavior to determine optimal segmentation scale. Others used a similar approach of assessing local variance to determine appropriate scale in pixel-based analysis [41], [42].

Another possible reason why the accuracy was higher as scale increased, particularly with the incorporation of texture measures, might have been the influence of an edge effect, even though the edge effect is smaller in object-based analysis compared to the moving window approach in pixel-based analysis [12]. At a fine scale, there are numerous small image objects, and therefore, the effect of the edge pixels is great. At coarser scales and with larger image objects, the ratio between edge pixels of an image object and the number of pixels in an image object is lower than that at finer scales. It is also likely that pixels that are edge pixels at small scales are integrated into the image objects at large scales and are included with the spatially adjacent classes.

The fact that fewer texture measures were chosen by the decision tree as the scale parameter became coarser corroborates the findings of the accuracy assessment. Based on our conclusion that a scale of 55–70 is most appropriate, the most suitable texture measures based on variable importance were $MENT$, $MCON$, and $MSTD$ (Table II). Because $MCON$ and $MDIS$ were strongly correlated at all scales, either $MCON$ or $MDIS$ could be chosen. If only one texture measure were to be used to reduce computing time, $MENT$ would be our choice, since it most frequently received a variable importance score of 100. Entropy is a measure of disorder, and contrast is a measure of spatial frequency or smoothness in an image [43]. In our high-resolution imagery, it is apparent that bare areas have considerably smoother texture (lower entropy values) than either shrub or grass patches (Fig. 6), and shrubs have a higher percentage of shadow and therefore higher spatial frequency than grasses.

To our best knowledge, there have been no other studies of the use of texture measures in object-based classification across multiple scales. Therefore, comparisons can only be made with texture studies in the pixel-based analysis using moving windows. However, with regard to the choice of texture measures, it appears that others found similar results, even with different imagery. In a study of sea ice using radar imagery, Clausi [28] reported that dissimilarity and contrast produced consistently strong classifications for all data sets. Shokr [36] determined that entropy and homogeneity were suited best for his study of sea ice with radar imagery. Baraldi and Parmiggiani [38] noted that contrast and energy (also called angular second moment) were most efficient for discriminating textural patterns in AVHRR imagery. Coburn and Roberts [10] used texture measures with digital aerial photography and found that entropy yielded the largest gains in classification accuracy.

Since image objects are very small at the fine scales, more edge pixels will be incorporated into the texture calculations, possibly skewing the results. This is the most likely reason that correlation coefficients often changed more erratically from one scale to the next below scale parameters of 25, while the rate of change in correlation coefficient was smaller as the scale parameter increased. Similar to our results, Clausi [28] and Barber and LeDrew [37] reported that contrast and dissimilarity were strongly correlated. On the other hand, Baraldi and Parmiggiani [38] determined that contrast and homogeneity were strongly and inversely correlated, while we observed an inverse but weak correlation.

A knowledge of correlation is useful in this type of analysis. Because decision trees are nonparametric in nature and correlated variables can be used as input, this tool may output a set of suitable features that are correlated, as we saw in our results. Since texture measures in object-based analysis are time-consuming to compute, one wants to keep the number of features to a minimum.

The class separability and accuracy analyses indicate that the inclusion of texture measures improved the results at nearly all segmentation scales. In general, classification accuracy was relatively high, both for using only RGB bands and RGB+texture bands. Therefore, the analyst has to decide whether a relatively small increase in accuracy is warranted by the inclusion of texture measures which have additional computing requirements. Using a workstation with two dual cores and 4 GB of RAM, a classification using only RGB bands was completed in 1–3 min, depending on the segmentation scales. Adding one texture measure increased the classification time to 55 min at scale 75 and to 3 h when three texture measures were used. With additional texture measures and a finer segmentation scale, some classifications took up to 6 h to complete. The image file size was 145 MB.

Due to the low flying height, the UAV imagery covered a relatively small footprint on the ground, but the number of pixels in the image was relatively high due to the 5-cm pixel resolution. Therefore, UAV image analysis can be even more computer intensive than the analysis of aerial photos from piloted aircraft. Given those limitations, it is preferable and less time consuming to use a decision tree analysis to find the fewest most suitable variables than to perform a series of classifications and/or class separability analyses to obtain the same results, particularly if multiple segmentation scales are analyzed.

While absolute scale parameters may have different values in different landscapes and for different flying heights, we expect that the approach of evaluating error rates and prediction success from decision trees, coupled with assessment of class separability and overall accuracy, can offer reliable guidance for selecting an image segmentation scale in other landscapes as well.

V. Conclusion

In this paper, we investigated texture measures at multiple scales in object-based analysis for the purpose of differentiating broad functional groups of vegetation in arid rangelands with

subdecimeter UAV imagery. Relatively coarser segmentation scales resulted in higher prediction success from the decision tree, better class separability, and higher accuracy than finer scales. The decision tree was a useful tool for narrowing down suitable texture measures for ease of computing, and the correlation analysis gave valuable insights into the changes in correlation of texture measure pairs across multiple scales.

The results demonstrate that UAVs are viable platforms for rangeland monitoring and that the drawbacks of low-cost off-the-shelf digital cameras can be overcome by including texture measures and using object-based image analysis which is highly suitable for very high resolution imagery. Our results will be incorporated into a rangeland monitoring protocol with unmanned aircraft. With the recent increase in high-resolution digital aerial cameras for piloted aircraft, the results have applicability in that field as well. Future studies will investigate the suitability of this analysis approach for other vegetation communities in arid rangelands and for more detailed vegetation classes. Additional studies are also needed to determine if the correlation trends we observed for the various texture measures across segmentation scales occur in other vegetation communities.

ACKNOWLEDGMENT

The authors would like to thank A. L. Slaughter for the assistance with field sampling and also the anonymous reviewers for their valuable comments.

REFERENCES

[1] T. D. Booth and P. T. Tueller, "Rangeland monitoring using remote sensing," *Arid Land Res. Manag.*, vol. 17, no. 4, pp. 455–467, Oct.–Dec. 2003.

[2] G. Zhou, C. Li, and P. Cheng, "Unmanned aerial vehicle (UAV) real-time video registration for forest fire monitoring," in *Proc. IGARSS*, Seoul, Korea, 2005, vol. 5, pp. 1803–1806.

[3] G. Zhou and D. Zang, "Civil UAV system for earth observation," in *Proc. IGARSS*, Barcelona, Spain, 2007, pp. 5319–5322.

[4] A. S. Laliberte, A. Rango, and J. E. Herrick, "Unmanned aerial vehicles for rangeland mapping and monitoring: A comparison of two systems," in *Proc. ASPRS Annu. Conf.*, Tampa, FL, 2007. unpaginated CD-ROM.

[5] A. Rango, A. S. Laliberte, C. Steele, J. E. Herrick, B. Bestelmeyer, T. Schmugge, A. Roanhorse, and V. Jenkins, "Using unmanned aerial vehicles for rangelands: Current applications and future potentials," *Environ. Pract.*, vol. 8, pp. 159–168, Jul. 2006.

[6] I. Epifanio and P. Soille, "Morphological texture features for unsupervised and supervised segmentations of natural landscapes," *IEEE Trans. Geosci. Remote Sens.*, vol. 45, no. 4, pp. 1074–1083, Apr. 2007.

[7] S. Ryherd and C. Woodcock, "Combining spectral and texture data in the segmentation of remotely sensed images," *Photogramm. Eng. Remote Sens.*, vol. 62, no. 2, pp. 181–194, 1996.

[8] M. A. Wulder, E. F. LeDrew, S. E. Franklin, and M. B. Lavigne, "Aerial image texture information in the estimation of northern deciduous and mixed wood forest leaf area index (LAI)," *Remote Sens. Environ.*, vol. 64, no. 1, pp. 64–76, Apr. 1998.

[9] S. E. Franklin, R. J. Hall, L. M. Moskal, A. J. Maudie, and M. B. Lavigne, "Incorporating texture into classification of forest species composition from airborne multispectral images," *Int. J. Remote Sens.*, vol. 21, no. 1, pp. 61–79, Jan. 2000.

[10] C. A. Coburn and A. C. B. Roberts, "A multiscale texture analysis procedure for improved forest stand classification," *Int. J. Remote Sens.*, vol. 25, no. 20, pp. 4287–4308, 2004.

[11] R. Haralick, K. Shanmugan, and I. Dinstein, "Textural features for image classification," *IEEE Trans. Syst., Man, Cybern.*, vol. SMC-3, no. 1, pp. 610–621, Nov. 1973.

[12] C. J. S. Ferro and T. A. Warner, "Scale and texture in digital image classification," *Photogramm. Eng. Remote Sens.*, vol. 68, no. 1, pp. 51–63, 2002.

[13] *Definiens Professional 5 User Guide*, Definiens, Munich, Germany, 2006.

[14] A. Lobo, K. Moloney, and N. Chiariello, "Fine scale mapping of a grassland from digitized aerial photography: An approach using image segmentation and discriminant analysis," *Int. J. Remote Sens.*, vol. 19, no. 1, pp. 65–84, 1998.

[15] M. E. Hodgson, J. R. Jensen, J. A. Tullis, K. D. Riordan, and C. M. Archer, "Synergistic use of Lidar and color aerial photography for mapping urban parcel imperviousness," *Photogramm. Eng. Remote Sens.*, vol. 69, no. 9, pp. 973–980, 2003.

[16] Q. Yu, P. Gong, N. Clinton, G. Biging, M. Kelly, and D. Schirokauer, "Object-based detailed vegetation classification with airborne high spatial resolution remote sensing imagery," *Photogramm. Eng. Remote Sens.*, vol. 72, no. 7, pp. 799–811, 2006.

[17] A. S. Laliberte, A. Rango, K. M. Havstad, J. F. Paris, R. F. Beck, R. McNeely, and A. L. Gonzalez, "Object-oriented image analysis for mapping shrub encroachment from 1937 to 2003 in Southern New Mexico," *Remote Sens. Environ.*, vol. 93, no. 1/2, pp. 198–210, Oct. 2004.

[18] A. S. Laliberte, E. L. Fredrickson, and A. Rango, "Combining decision trees with hierarchical object-oriented image analysis for mapping arid rangelands," *Photogramm. Eng. Remote Sens.*, vol. 73, no. 2, pp. 197–207, 2007.

[19] E. Ivits and B. Koch, "Object-oriented remote sensing tools for biodiversity assessment: A European approach," in *Proc. 22nd EARSeL Symp.*, Prague, Czech Republic, 2002, pp. 8–16.

[20] D. Flanders, M. Hall-Beyer, and J. Pereverzoff, "Preliminary evaluation of eCognition object-based software for cut block delineation and feature extraction," *Can. J. Remote Sens.*, vol. 29, no. 4, pp. 441–452, 2003.

[21] J. Radoux and P. Defourny, "A quantitative assessment of boundaries in automated forest stand delineation using very high resolution imagery," *Remote Sens. Environ.*, vol. 110, no. 4, pp. 468–475, Oct. 2007.

[22] L. Wang, W. P. Sousa, and P. Gong, "Integration of object-based and pixel-based classification for mapping mangroves with IKONOS imagery," *Int. J. Remote Sens.*, vol. 25, no. 24, pp. 5655–5668, Dec. 2004.

[23] M. Kim and M. Madden, "Determination of optimal scale parameter for alliance-level forest classification of multispectral Ikonos images," in *Proc. 1st Int. Conf. OBIA, Int. Arch. Photogramm. Remote Sens. Spat. Inf. Sci.*, 2006. unpaginated CD-ROM, 4 p.

[24] M. S. Chubey, S. E. Franklin, and M. A. Wulder, "Object-based analysis of Ikonos-2 imagery for extraction of forest inventory parameters," *Photogramm. Eng. Remote Sens.*, vol. 72, no. 4, pp. 383–394, 2006.

[25] D. G. Blumberg and G. Zhu, "Using a hierarchical multi-resolution mechanism for the classification and semantic extraction of landuse maps for Beer-Sheva, Israel," *Int. J. Remote Sens.*, vol. 28, no. 15, pp. 3273–3289, 2007.

[26] K. Johansen, S. Phinn, I. Dixon, M. Douglas, and J. Lowry, "Comparison of image and rapid field assessments of riparian zone condition in Australian tropical savannas," *For. Ecol. Manag.*, vol. 240, no. 1–3, pp. 42–60, Mar. 2007.

[27] L. Bruzzone and L. Carlin, "A multilevel context-based system for classification of very high spatial resolution images," *IEEE Trans. Geosci. Remote Sens.*, vol. 44, no. 9, pp. 2587–2600, Sep. 2006.

[28] D. A. Clausi, "An analysis of co-occurrence texture statistics as a function of grey level quantization," *Can. J. Remote Sens.*, vol. 28, no. 1, pp. 45–62, 2002.

[29] L. Breiman, J. H. Friedman, R. A. Olshen, and C. J. Stone, *Classification and Regression Trees*. Belmont, CA: Wadsworth, 1984.

[30] R. S. DeFries, M. Hansen, J. R. G. Townshend, and R. Sohlberg, "Global land cover classifications at 8 m spatial resolution: The use of training data derived from Landsat imagery in decision tree classifiers," *Int. J. Remote Sens.*, vol. 19, no. 16, pp. 3141–3168, 1998.

[31] R. Lawrence, A. Bunn, S. Powell, and M. Zambon, "Classification of remotely sensed imagery using stochastic gradient boosting as a refinement of classification tree analysis," *Remote Sens. Environ.*, vol. 90, no. 3, pp. 331–336, Apr. 2004.

[32] N. Thomas, C. Hendrix, and R. G. Congalton, "A comparison of urban mapping methods using high-resolution digital imagery," *Photogramm. Eng. Remote Sens.*, vol. 69, no. 9, pp. 963–972, 2003.

[33] J. A. Tullis and J. R. Jensen, "Expert system house detection in high spatial resolution imagery using size, shape, and context," *Geocarto Int.*, vol. 18, no. 1, pp. 5–15, Mar. 2003.

[34] U. C. Benz, P. Hoffmann, G. Willhauck, I. Lingenfelder, and M. Heynen, "Multi-resolution, object-oriented fuzzy analysis of remote sensing data for GIS-ready information," *ISPRS J. Photogramm.*, vol. 58, no. 3/4, pp. 239–258, Jan. 2004.

[35] D. Steinberg and P. Colla, *CART—Classification and Regression Trees*. San Diego, CA: Salford Syst., 1997.

[36] M. Shokr, "Evaluation of second-order texture parameters for sea ice classification from radar images," *J. Geophys. Res.*, vol. 96, no. C6, pp. 10 625–10 640, Jun. 1991.
[37] D. G. Barber and E. F. LeDrew, "SAR sea ice discrimination using texture statistics: A multivariate approach," *Photogramm. Eng. Remote Sens.*, vol. 57, no. 4, pp. 385–395, 1991.
[38] A. Baraldi and F. Parmiggiani, "An investigation of the textural characteristics associated with gray level cooccurrence matrix statistical parameters," *IEEE Trans. Geosci. Remote Sens.*, vol. 33, no. 2, pp. 293–304, Mar. 1995.
[39] R. R. Sokal and F. J. Rohlf, *Biometry: The Principles and Practice of Statistics in Biological Research*. New York: Freeman, 1995.
[40] R. G. Congalton, "A review of assessing the accuracy of classifications of remotely sensed data," *Remote Sens. Environ.*, vol. 37, no. 1, pp. 35–46, Jul. 1991.
[41] C. E. Woodcock and A. H. Strahler, "The factor of scale in remote sensing," *Remote Sens. Environ.*, vol. 21, no. 3, pp. 311–332, Apr. 1987.
[42] D. J. Marceau, D. J. Gratton, R. A. Fournier, and J.-P. Fortin, "Remote sensing and the measurement of geographical entities in a forested environment. 2. The optimal spatial resolution," *Remote Sens. Environ.*, vol. 49, no. 2, pp. 105–117, Aug. 1994.
[43] M. Herold, X. Liu, and K. C. Clarke, "Spatial metrics and image texture for mapping urban land use," *Photogramm. Eng. Remote Sens.*, vol. 69, no. 9, pp. 991–1001, 2003.

Andrea S. Laliberte received the B.S. degree in natural resource science from the University College of the Caribou, Kamloops, BC, Canada, and the M.S. degree in rangeland resources and the Ph.D. degree in forest resources from Oregon State University, Corvallis.

She is currently a Remote Sensing Scientist with the Jornada Experimental Range, New Mexico State University, Las Cruces, and an Adjunct Professor with the Geography Department, New Mexico State University. Her research focuses on developing remote sensing techniques for rangeland applications using hyperspatial imagery and object-oriented image analysis. Her current research is focused on incorporating unmanned aircraft system imagery for mapping and monitoring arid land vegetation.

Albert Rango received the B.S. and M.S. degrees in meteorology from Pennsylvania State University, University Park, and the Ph.D. degree in watershed management from Colorado State University, Fort Collins.

He is currently a Research Hydrologist with the USDA-ARS Jornada Experimental Range, New Mexico State University, Las Cruces. He has over 350 publications in the fields of remote sensing, rangeland applications, watershed management, and snow hydrology.

Dr. Rango is a past President of the IAHS International Commission on Remote Sensing, the American Water Resources Association, and the Western Snow Conference. He was selected as the Agricultural Research Service's Distinguished Senior Research Scientist of the Year in 2000.